ELSEVIER

Catalysis Today 79–80 (2003) 453–464

CATALYSIS TODAY

www.elsevier.com/locate/cattod

Effects of temperature distribution on the catalytic pyrolysis of polystyrene waste in a swirling fluidized-bed reactor

Chan-Gi Lee [a], Yong-June Cho [a], Pyung-Seob Song [a], Yong Kang [a,*], Jun-Sik Kim [b], Myoung-Jae Choi [b]

[a] *School of Chemical Engineering, Chungnam National University, Daeduk Science Town, Taejon 305-764, South Korea*
[b] *Advanced Chemical Technology Division, KRICT, Taejon 305-600, South Korea*

Abstract

A swirling fluidized-bed reactor (0.0508 m ID and 1.5 m in height) has been developed to recover the styrene monomer and valuable chemicals effectively from the polystyrene waste, since it can control the residence time of the feed materials and enhance the uniformity of the temperature distribution. To increase the selectivity and yield of styrene monomer in the product, catalyst such as Fe_2O_3, BaO or HZSM-5 (Si/Al = 30) have been used. Effects of temperature, volume flow rate of gas, pyrolysis time and the ratio of swirling gas to the amount of primary fluidizing gas on the yields of oil product as well as styrene monomer have been determined. Effects of operating variables on the temperature distributions and their fluctuations in the radial as well as axial directions have been also examined to analyze the effects of temperature distributions and their fluctuations on the catalytic pyrolysis of polystyrene waste in the swirling fluidized-bed reactor. It has been found that the reaction time and temperature can be reduced profoundly by adding the solid catalyst. The swirling fluidization mode makes the temperature fluctuations more periodic and persistent, which can increase the uniformity of temperature distribution by reducing the temperature gradient in the reactor. The yields of styrene monomer as well as oil products have increased with increasing the ratio of swirling gas (V_2/V_1), but exhibited their maximum values with increasing the total volume flow rate of gas.

Keywords: Recovery of styrene monomer; Pyrolysis; Polystyrene waste; Catalyst; Swirling fluidized-bed; Chaos analysis; Temperature distribution

1. Introduction

One of the promising alternative to dumping or incineration for the treatment of plastic waste such as polystyrene can be pyrolysis to recover the monomer or other valuable chemicals. The recycling to fuel oils from the waste polymers has been attractive and sometimes commercially operated. However, the fuel oils thus recovered are producing lots of carbon dioxide when burnt as fuels. Therefore, several investigations have been focused on the recovery of monomers from its polymers [1–3]. It can be understood that the temperature distribution and heat transfer in the reactor are important factors to determine the reactor performance as well as the yields of oil and monomer in the pyrolysis reactor, since the pyrolysis of polymer plastic waste has to be carried out in the high temperature. In addition, the residence time and distribution of polymers in the reactor can affect the product distribution recovered. The more uniform temperature distribution can be achieved by generating the swirling flow pattern of gas–solid mixture

* Corresponding author. Tel.: +82-42-821-5683; fax: +82-42-822-8995.
E-mail address: kangyong@hanbat.cnu.ac.kr (Y. Kang).

0920-5861/03/$ – see front matter © 2003 Elsevier Science B.V. All rights reserved.
doi:10.1016/S0920-5861(03)00060-9

Nomenclature

W_f	weight of feed material (g)
W_o	weight of obtained oil (g)
W_{SM}	weight of obtained styrene monomer (g)
Y_{oil}	yield of oil (wt.%)
Y_{SM}	yield of styrene monomer (wt.%)

by means of the injection of the swirling gas into the dense bed of bed material. The swirling fluidized-bed has been recognized as a scheme to control the residence time distributions of feed materials as well as gas products in the reactor [4–10]. However, the thermo-physical behaviors of gas–solid fluidized-bed reactor are highly complicated and sometimes random owing to the irregular contacting and flow behaviors of gas and solid. The resultant bubbling and complex flow behavior of multiphase flow systems have been successfully interpreted by analyzing the fluctuations of their state variables such as temperature [11–13].

In the present study, thus, the swirling fluidized-bed reactor has been proposed to recover the styrene monomer and valuable chemicals effectively from the polystyrene waste. Effects of catalyst and operating variables on the yields of oil product as well as styrene monomer have been determined. In addition, temperature distributions and fluctuations have been examined, to analyze the effects of them on the reaction. The temperature fluctuations have been analyzed by means of phase space portraits and correlation dimension.

2. Analysis of temperature fluctuations

2.1. Phase space portraits

The multidimensional phase space portraits can be constructed from the time series of pressure fluctuations by means of the time delay method [14]. That is, the experimentally obtained time series signal, $X(t)$, is digitized with a time step of Δt; the resultant $(m+1)$ values of the signal, $X(i\Delta t)$, are stored for $i = 0, 1, 2, \ldots, m$. Thus, the vector time series is defined as

$$Z_i(t) = [X(i\Delta t), X(i\Delta t + \tau), \ldots, X(i\Delta t + (p-1)\tau)], \quad i = 0, 1, 2, \ldots, [m - (p-1)k] \quad (1)$$

where $\tau = k\Delta t$, $k = 1, 2, 3, \ldots$ and p is the dimension of the vector, $Z(t)$. Therefore, moving along with time t, a series of p-dimensional vectors representing the p-dimensional portrait of the system can be obtained. Occasionally, p is referred to as the embedded phase space dimension of the reconstructed trajectory of attractor. Actually, if $\tau = 1$ and $p = 3$, the state vectors presenting one orbit of attractor is constructed from the experimentally measured time series signals as $Z_1 = [X_1, X_2, X_3]^T$, $Z_2 = [X_2, X_3, X_4]^T$, etc. Thus the number of elements, p, of the state vector is equal to the number of coordinates in the reconstructed state space. In this way two-dimensional reconstructed attractor of a time series can be obtained.

2.2. Correlation dimension

To estimate the correlation dimension of the time series $X(t)$, the trajectories of them reconstructed by resorting to time embedding have been used. From the trajectories of the vector time series the correlation integral (the space correlation function) of the process, $C(r)$, is defined as [15,16]

$$C(r) = \lim_{m\to\infty} \frac{1}{m^2}[\text{number of pairs } (i, j) \text{ whose distance } |Z_i(t) - Z_j(t)| < r] \quad (2)$$

Formally,

$$C(r) = \lim_{m\to\infty} \frac{1}{m^2} \sum_{i=1}^{m}\sum_{j=1}^{m} H[r - |Z_i(t) - Z_j(t)|], \quad i \neq j \quad (3)$$

where m is the number of data points, and H Heaviside function,

$$H[r - |Z_i(t) - Z_j(t)|] = \begin{cases} 1 & \text{if } r > |Z_i(t) - Z_j(t)|, \\ 0 & \text{otherwise} \end{cases} \quad (4)$$

The correlation integral, $C(r)$, has been found to be a power function of r for small r's:

$$C(r) = kr^{D_c} \quad (5)$$

The slope of the plot of $\ln C(r)$ vs. $\ln r$ is an estimate of D_c which is termed as the correlation dimension, for the given embedded space dimension, p.

3. Experimental

Experiments were carried out in a stainless steel fluidized-bed reactor whose diameter was 0.0508 and 1.5 m in height, respectively, as can be seen in Fig. 1 [17,18]. The freeboard region was made of 0.102 m ID stainless steel tube. The dried, filtered and compressed nitrogen gas was injected into the reactor through the perforated-type distributor installed between the main column section and the distributor box, after preheating by means of preheater installed in the main gas feed line. The distributor contained 27 holes with triangular pitches and was covered with 400 mesh screen for preventing from bed material weeping. The diameter of each hole was 6 mm. Sand particles whose density and mean diameter were 2500 kg/m^3 and 240 μm, respectively, were used as the bed materials. The swirling gas (nitrogen) was

Table 1
Property of catalysts

Catalyst	Density (g/cm^3)	d_p (μm)	U_{mf} (m/s)	U_t (m/s)
Fe_2O_3	5.12	85.62	0.033	0.6824
BaO	5.72	150	0.1136	1.3517
HZSM-5	2.6	160	0.04	0.88

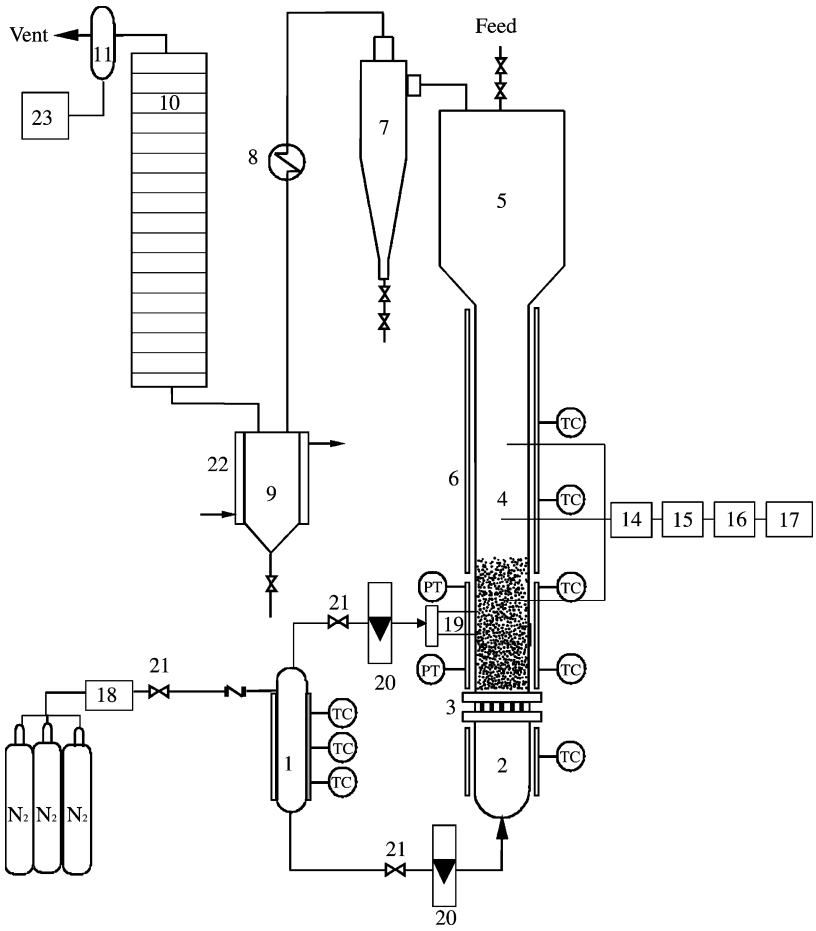

Fig. 1. Experimental apparatus: (1) pre-heater; (2) distributor box; (3) distributor; (4) F-bed reactor; (5) freeboard; (6) electric heater; (7) cyclone; (8) heat exchanger; (9) condenser; (10) mist filter; (11) gas sample bag; (12) gas meter; (13) temperature sensor; (14) amplifier; (15) low-pass filter; (16) A/D converter; (17) computer; (18) regulator; (19) swirling gas port; (20) flowmeter; (21) control valve; (22) water jacket; (23) GC.

Table 2
Ultimate analysis and calorific value of waste expanded polystyrene

Feed material	Calorific value (cal/g)	Element (wt.%)				
		Carbon	Hydrogen	Nitrogen	Sulfur	Oxygen
EPSW	9507	91.50	7.62	0.04	0.03	0.81

fed to the reactor tangentially at the wall of the reactor, to formulate the swirling motion interior of the reactor. The ratio of swirling gas was in the range of 0–0.5. The swirling gas also preheated by means of preheater. The height of the swirling gas injection port was 0.05 m from the distributor. Five pressure taps were mounted flush with the reactor wall in an interval of 0.2 m. The temperature sensors were installed in the dimensionless radial coordinate (r/R) of 0, 0.3, 0.6 and 0.9 and 0, 0.25, 0.5, 0.75 and 1 in the dimensionless axial coordinate (h/H). Catalysts such as Fe_2O_3, BaO or HZSM-5 were used to enhance the conversion of the reaction. The properties of catalysts were summarized in Table 1. Expanded polystyrene waste (EPSW) was used as a feed material. The ultimate analysis and calorific value of EPSW were summarized in Table 2. The EPSW was melted at 250 °C prior to be injected into the reactor, to be made as particles with a mean diameter of 1 mm. The catalyst was mixed with the feed material during this process in a given amount [18]. Fifty grams of feed material was fed to the reactor in a given operating condition. The yield of oil product or styrene monomer was determined by the following equations:

$$Y_{\text{oil}} = \frac{W_{\text{o}}}{W_{\text{f}}} \times 100,$$
$$Y_{\text{SM}} = \frac{W_{\text{SM}}}{W_{\text{f}}} \times 100 = \frac{W_{\text{SM}} \times Y_{\text{oil}}}{W_{\text{o}}} \times 100 \quad (6)$$

The outlet gas which was obtained at the gas detection port was analyzed by means of on-line gas analyzer (GC-MS, HP-5890 plus, column; DB-1HT; GC-TDC; GC-FID). The temperature fluctuations

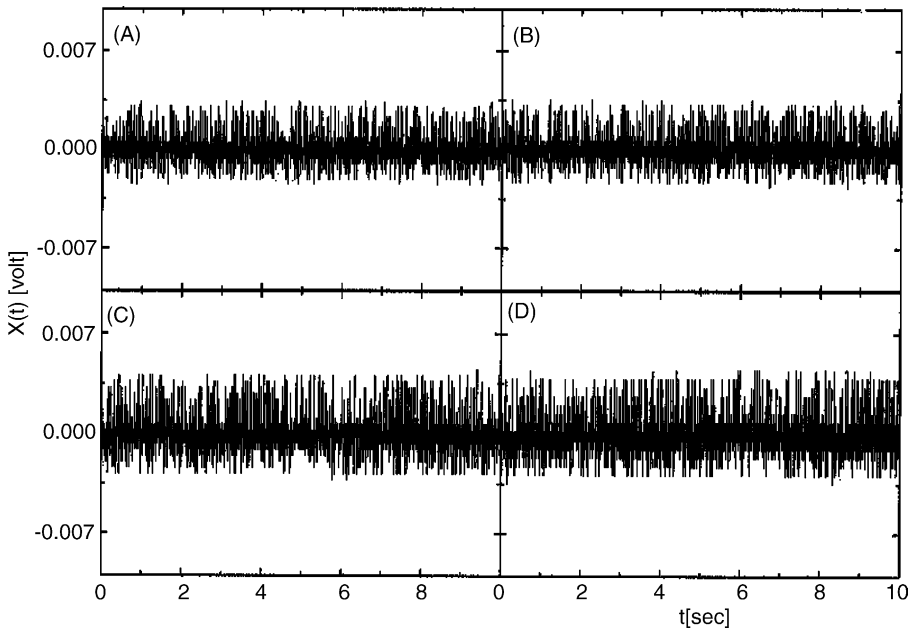

Fig. 2. Typical example of temperature fluctuations in a swirling fluidized-bed reactor ($h/H = 0.5$): (A) $V_2/V_1 = 0, r/R = 0.3$; (B) $V_2/V_1 = 0.1, r/R = 0.3$; (C) $V_2/V_1 = 0.1, r/R = 0.6$; (D) $V_2/V_1 = 0.1, r/R = 0.9$.

were measured and recorded by temperature sensors and transducers after the gas–solid flow attained a steady state fluidization condition. The temperature sensor was a semiconductor type (Coppel electronics) that has enough fast response time to measure the dynamic temperature fluctuations in the column. The output voltage from the temperature transducer, which is proportional to the temperature fluctuations, was processed by means of a data acquisition system (Data Precision Model, D-6000) and a personal computer. The voltage–time signals, corresponding to the temperature–time signals, were sampled at a rate of 0.005 s and stored in the data acquisition system. The total acquisition time was 15 s having 3000 data points. This combination of sampling rate and time can detect the full spectrum of hydrodynamic signals (200 Hz) in multiphase flow system [11,19].

4. Results and discussions

Typical example of temperature fluctuations can be seen in Fig. 2, with variations of the swirling gas ratio and radial position in the reactor. In this figure, the temperature fluctuations are more complicated by introducing the swirling gas into the reactor. This can be due to the generation of swirling flow motion in the reactor. Since the swirling gas has been injected into the dense bed area of the fluidized-bed reactor, it can easily lead to the suitable bed expansion by way of swirling flow pattern of gas–bed material mixture. Note that the temperature fluctuations also become more complicated with increasing the radial position (r/R). The temperature fluctuations can be more effectively visualized by means of phase space portraits. To construct the phase space portraits from the

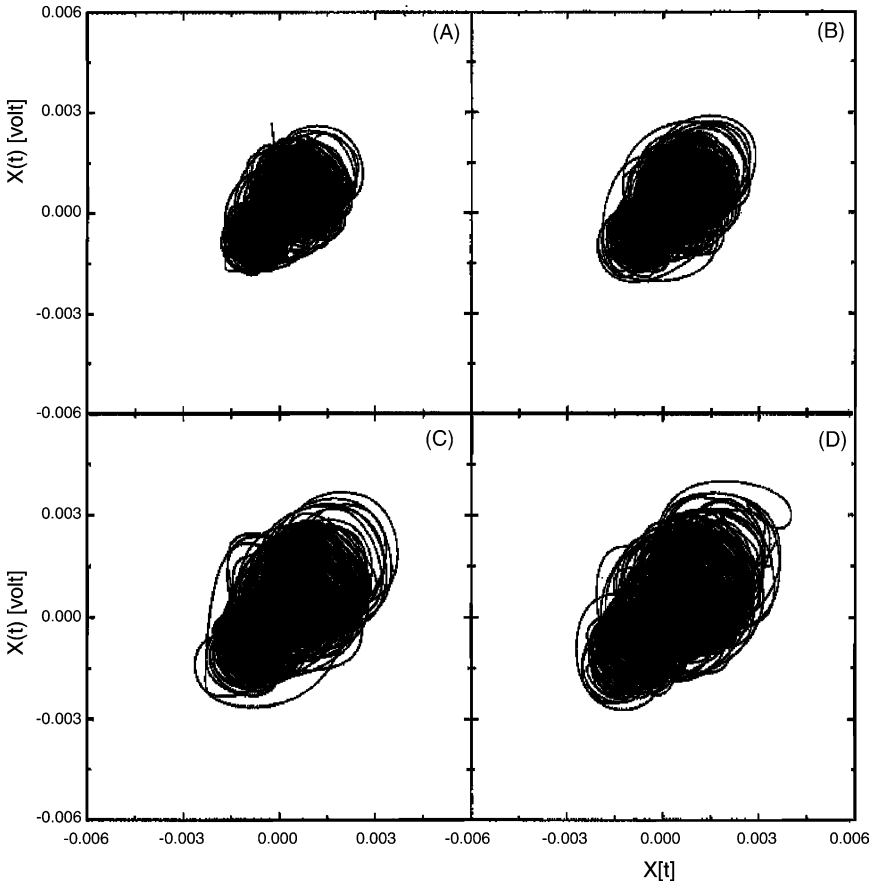

Fig. 3. Typical example of phase space portraits of temperature fluctuations in a swirling fluidized-bed reactor ($h/H = 0.5$): (A) $V_2/V_1 = 0, r/R = 0.3$; (B) $V_2/V_1 = 0.1, r/R = 0.3$; (C) $V_2/V_1 = 0.1, r/R = 0.6$; (D) $V_2/V_1 = 0.1, r/R = 0.9$.

temperature fluctuation signals, the value of optimum time lag has been chosen as 0.005 s, corresponding to the first minimum in the mutual information function [14,19]. Because, the mutual information function gives the unique feature in predicting the relation between the discrete data sets. Effects of the swirling gas injection and radial position on the strange attractor of temperature fluctuations in the phase space can be seen in Fig. 3. In this figure, the attractor is more scattered and complex by introducing the swirling gas and increasing the radial coordinate. It has been understood that the size, location and character of the loops in the trajectories help identify the underlying systems with their physical events [16,19]. In comparing the traces with the flow behavior of gas–solid mixture in the reactor, it can be indicated that the symmetry of the attractor can be corresponding to the periodic component of the temperature fluctuations and thus to the periodic flow behavior of gas–solid mixture in the reactor. Therefore, it can be stated that the flow behavior of gas–solid mixture becomes more complicated by introducing the swirling gas into the reactor or by increasing the dimensionless radial coordinate. For the quantitative analysis of the thermo-physical flow behavior in the reactor, the correlation dimension of temperature fluctuations have been calculated [16,19]. Typical example of correlation integral can be seen in Fig. 4. Effects of swirling gas ratio (V_2/V_1) and radial position in the reactor (r/R) on the values of correlation dimension of temperature fluctuations can be seen in Fig. 5. As can be expected, the value of D_c increases with increasing V_2/V_1 (Fig. 5A) or dimensionless radial coordinate (Fig. 5B). The quantitative explanation on the thermo-physical flow behavior of gas–solid mixture in the reactor is possible by means

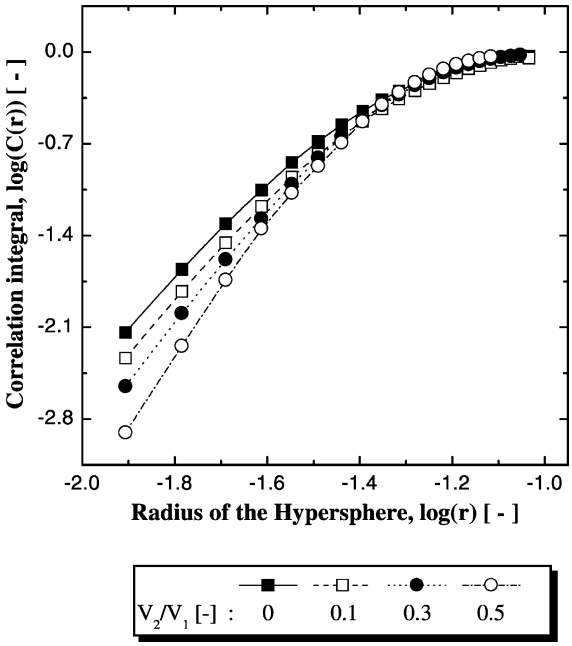

Fig. 4. Typical example of correlation analysis of temperature fluctuations in a swirling fluidized-bed reactor ($r/R = 0, h/H = 0.5$): (■) $V_2/V_1 = 0$; (□) $V_2/V_1 = 0.1$; (●) $V_2/V_1 = 0.3$; (○) $V_2/V_1 = 0.5$.

of the value of correlation dimension. The temperature at a given axial and radial position has been determined from the mean value of temperature fluctuations at that point. The temperature distributions in the radial as well as axial directions can be seen in Fig. 6. Note in Fig. 6A that the temperature in the zone adjacent to the wall of the reactor shows higher value than that in the center area. This can be due to that the pyrolysis is endothermic reaction. Also, note that the

Table 3
Comparison of selectivity among thermal and catalytic pyrolysis of polystyrene foams at 450 °C without swirling gas[a]

	Fe_2O_3, EPSW (95.2 wt.%)	BaO, EPSW (94.9 wt.%)	SiO_2/Al_2O_3, EPSW (92 wt.%)	Thermal, EPSW (90 wt.%)
Selectivity (%)				
SM	75.4	71.1	65.4	64
SD	12.8	13.7	8.4	4.69
ST	2.4	3.2	2.8	4.52
α-MS	5.41	7.4	4.32	5.19
T	1.14	1.3	5.6	0.96
B	0.02	0.1	0.86	0.06
EB	0.2	3.5	8.2	1.28

[a] SM: styrene monomer; SD: styrene dimmer; α-MS: α-methyl styrene; T: toluene; B: benzene; EB: ethyl benzene.

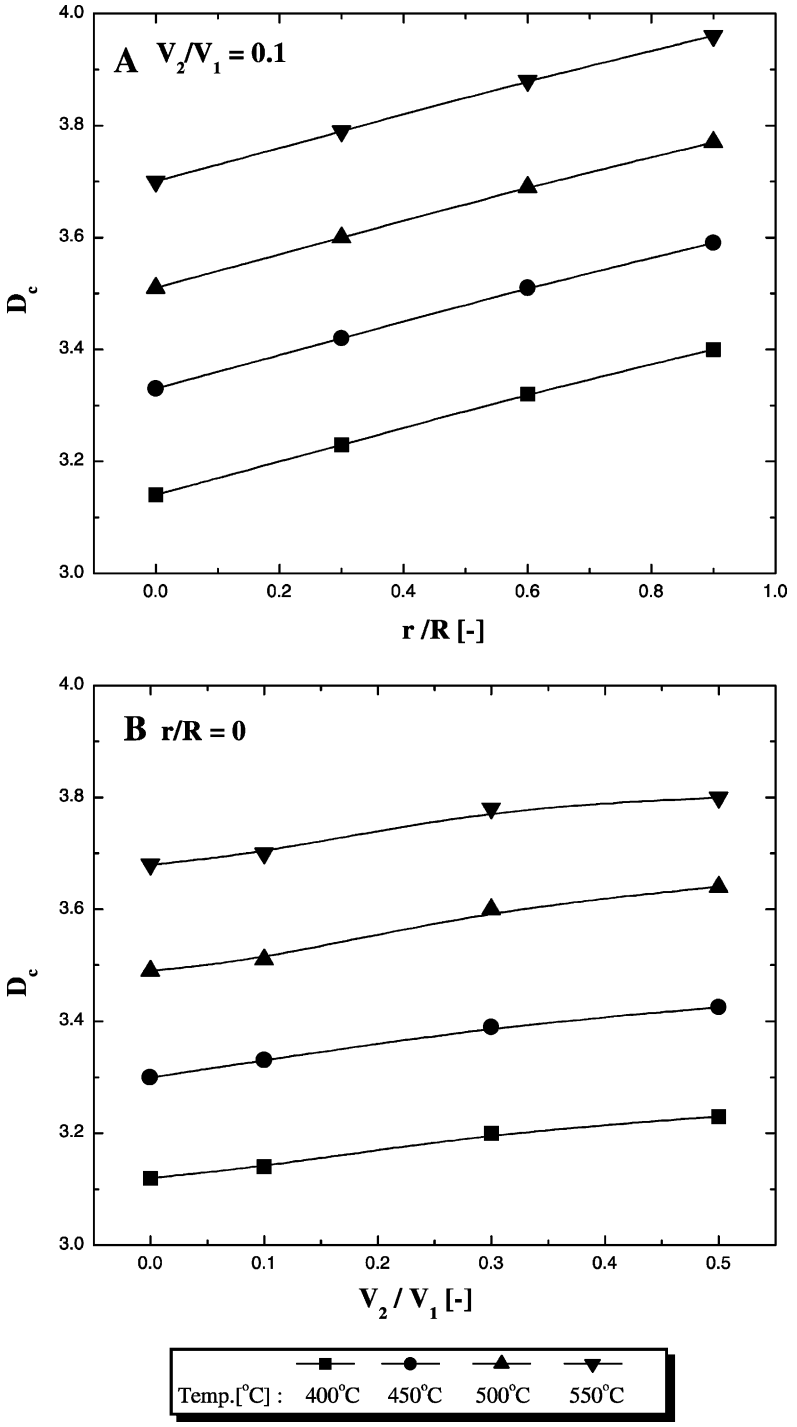

Fig. 5. Effects of radial position (A) and swirling gas ratio (B) on the correlation dimension of temperature fluctuations in a swirling fluidized-bed reactor: (■) $T = 400\,^{\circ}C$; (●) $T = 450\,^{\circ}C$; (▲) $T = 500\,^{\circ}C$; (▼) $T = 550\,^{\circ}C$.

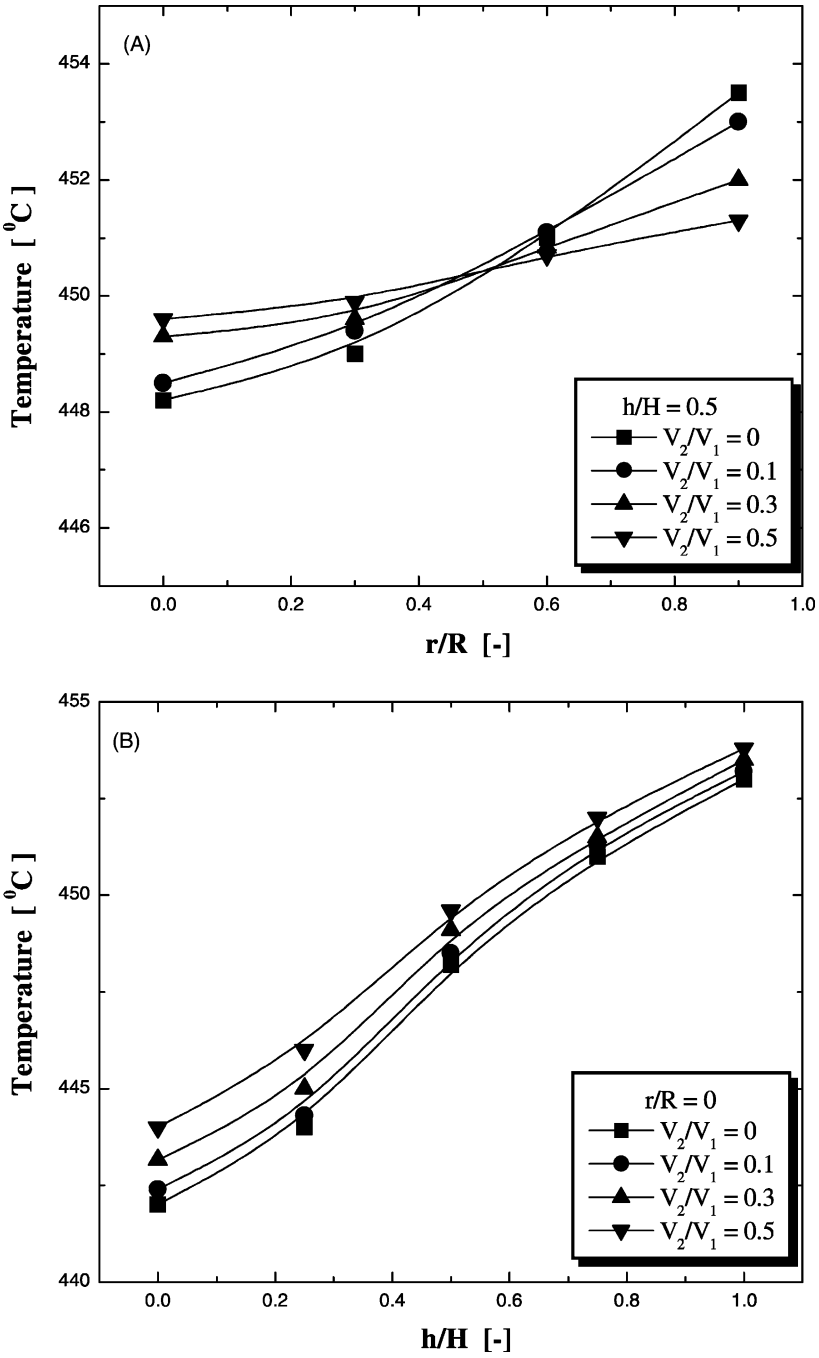

Fig. 6. Radial (A) and axial (B) temperature distributions in a swirling fluidized-bed reactor. A ($h/H = 0.5$): (■) $V_2/V_1 = 0$; (●) $V_2/V_1 = 0.1$; (▲) $V_2/V_1 = 0.3$; (▼) $V_2/V_1 = 0.5$. B ($r/R = 0$): (■) $V_2/V_1 = 0$; (●) $V_2/V_1 = 0.1$; (▲) $V_2/V_1 = 0.3$; (▼) $V_2/V_1 = 0.5$.

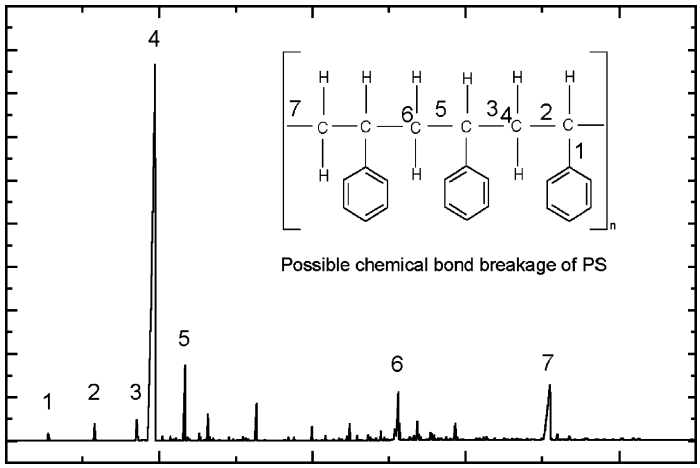

Fig. 7. Gas chromatogram of liquid products from polystyrene pyrolysis: (1) benzene; (2) toluene; (3) ethyl benzene; (4) styrene monomer; (5) α-methyl styrene; (6) styrene dimer; (7) styrene trimer.

radial temperature gradient decreases considerably with increasing the amount of swirling gas. This can be attributed to that the heat transfer would be enhanced due to the vigorous contact and mixing in the reactor by introducing the swirling gas [4,6,20]. The mean temperature increases gradually with increasing the axial coordinate in the bed (Fig. 6B). Since the products or intermediate materials rise in the bed as a gas phase with nitrogen gas, relatively small amount of heat would be required in the higher part of the bed.

Typical example of gas chromatogram of liquid products obtained from polystyrene waste by pyrolysis can be seen in Fig. 7. Note that the product is mainly composed of aromatics such as monomer, dimmer and trimer which are produced by breaking the main chain of the polystyrene [17,21]. Effects of catalyst on the yield of oil in a swirling fluidized-bed reactor can be seen in Fig. 8. This figure shows that Fe_2O_3 can be more effective to increase the yield of oil than BaO or HZSM-5. In this figure, 90 wt.% of Y_{oil} has been obtained in the reactor without catalyst and swirling gas during the reaction of 30 min (Fig. 8A), while it can be increased up to 92 wt.% for 26 min by injection of swirling gas ($V_2/V_1 = 0.3$). However, the addition of catalyst cannot only reduce the reaction time but also increase the Y_{oil} level [22,23]. That is to say, almost 95 wt.% of Y_{oil} can be achieved within 16 min by adding Fe_2O_3 catalyst in the fluidized-bed reactor, when the swirling gas ratio is 0.3. Other catalysts such as BaO or HZSM-5 also increases the Y_{oil} level and reduces the reaction time, but, in this case, the Y_{oil} level is lower than that of Fe_2O_3. Comparison of selectivity among catalytic and thermal pyrolysis and effects of catalyst on the selectivity of products have been summarized in Table 3. In this table, the selectivity of styrene monomer shows higher value in using Fe_2O_3 catalyst than that in using BaO, SiO_2/Al_2O_3 or without catalyst. Effects of swirling gas ratio (V_2/V_1) on the values of Y_{oil} and Y_{SM} can be seen in Fig. 9. The values of yields of oil and styrene monomer increase almost linearly with increasing the ratio of swirling gas. This can be due to the increases of residence time of gas in the reactor by means of swirling flow motion. It has been reported that the reaction time of thermal decomposition of plastics in the fluidized-bed reactor is only several seconds, thus, the residence time and its distribution can affect the yield of the product as well as product distribution [7,9,20]. It is interesting to note that the values of correlation dimension of temperature fluctuations increase almost linearly with increasing V_2/V_1 (Fig. 5B). Also note that the temperature gradient decreases profoundly in the reactor with increasing V_2/V_1 (Fig. 6A). Therefore, it is reasonable to state that the values of Y_{oil} and Y_{SM} can be increased due to the more uniform temperature condition by increasing the sufficient mixing, contacting and thus heat transfer, which can be realized by introducing the swirling gas. Although

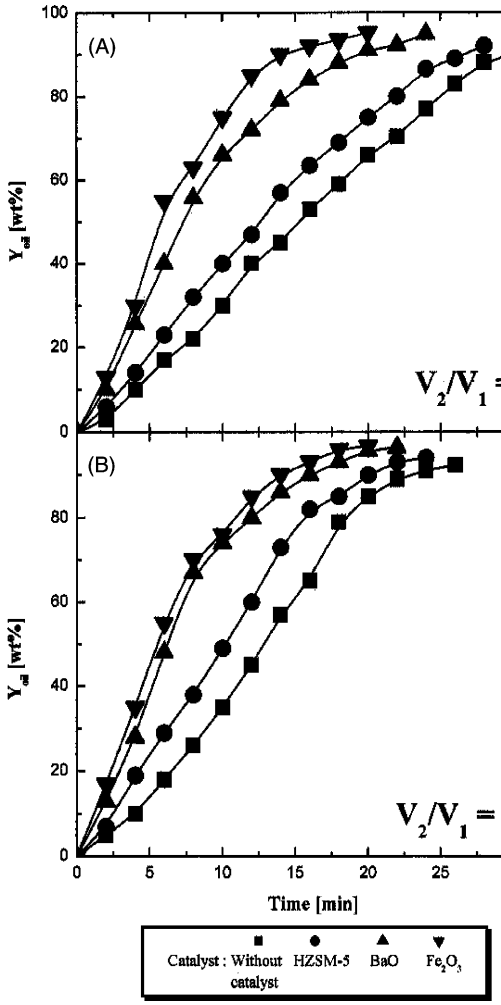

Fig. 8. Effects of catalyst on the yield of oil in a swirling fluidized-bed reactor ($T = 450\,^{\circ}C$, $V_o = 3.6\,m^3/s$): (■) without catalyst; (●) HZSM-5; (▲) BaO; (▼) Fe_2O_3.

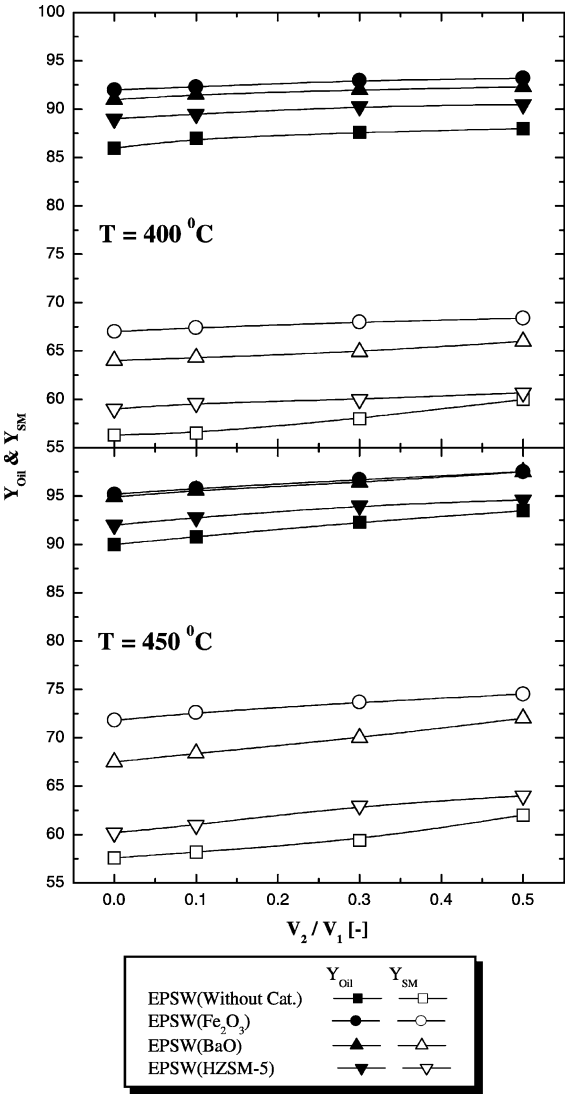

Fig. 9. Effects of swirling gas amount on the yield of oil and styrene monomer in a swirling fluidized-bed reactor ($V_o = 3.6\,m^3/s$). Y_{oil}: (■) EPSW (without catalyst); (●) EPSW (Fe_2O_3); (▲) EPSW (BaO); (▼) EPSW (HZSM-5). Y_{SM}: (□) EPSW (without catalyst); (○) EPSW (Fe_2O_3); (△) EPSW (BaO); (▽) EPSW (HZSM-5).

the values of V_2/V_1 is changed, the total gas volume flow rate, V_o, has been maintained in a given value.

Effects of total gas amounts (V_o) on the yields of oil product and styrene monomer can be seen in Fig. 10. Note that the values of Y_{oil} and Y_{SM} attain their maxima with increasing the total gas amount. This can be explained that in the lower range of V_o, the fluidization of bed materials becomes more vigorous with increasing V_o, but in the higher range of V_o, the increase of V_o leads to the higher bed expansion, which results in the significant decreases of holdup of bed materials. This can directly decrease the heat transfer and mixing phenomena in the fluidized-bed reactor. Thus, the values of Y_{oil} and Y_{SM} tend to decrease with a further increase of V_o. It has been understood that the heat transfer coefficient in gas–solid fluidized-bed reactor exhibits a maximum value with increasing gas amount or gas flow rate [24]. The gas volume flow rate corresponding to the maximum values of Y_{oil} and

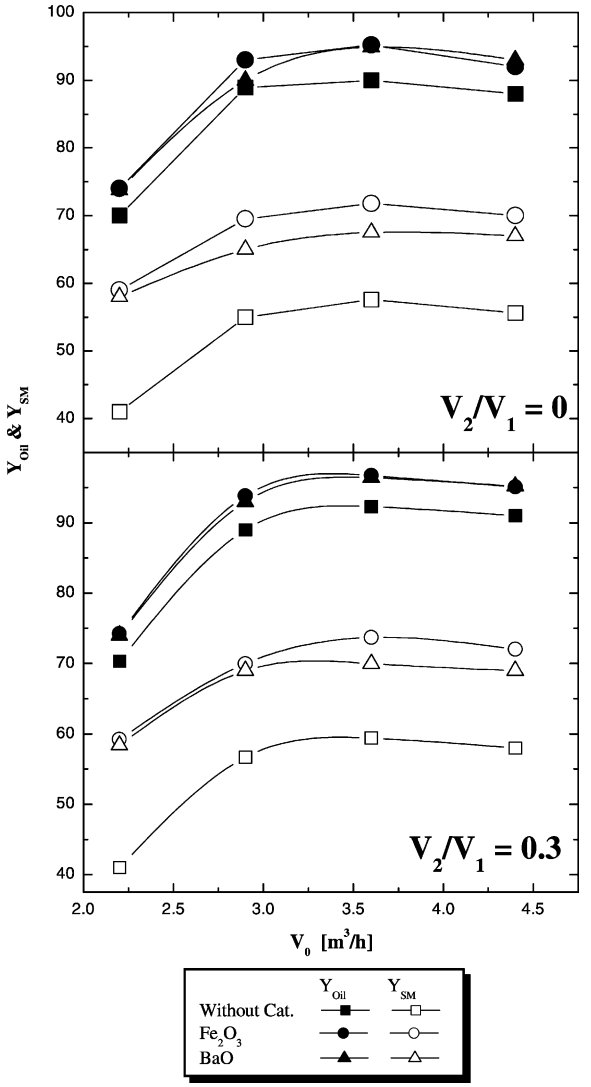

Fig. 10. Effects of total gas amount on the yield of oil and styrene monomer in a swirling fluidized-bed reactor ($T = 450\,^{\circ}C$). Y_{oil}: (■) without catalyst; (●) Fe_2O_3; (▲) BaO. Y_{SM}: (□) without catalyst; (○) Fe_2O_3; (△) BaO.

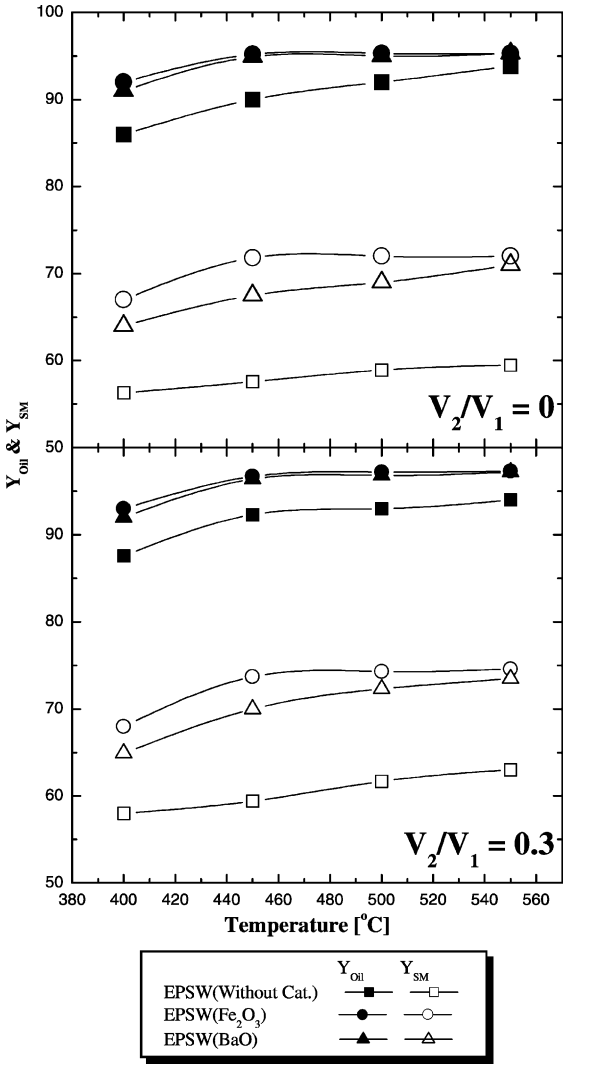

Fig. 11. Effects of temperature on the yield of oil and styrene monomer in a swirling fluidized-bed reactor ($V_o = 3.6\,m^3/s$). Y_{oil}: (■) EPSW (without catalyst); (●) EPSW (Fe_2O_3); (▲) EPSW (BaO). Y_{SM}: (□) EPSW (without catalyst); (○) EPSW (Fe_2O_3); (△) EPSW (BaO).

Y_{SM} is $3.6\,m^3/h$ (Fig. 10). Therefore, this value can be a optimum within this experimental conditions. Effects of reaction temperature on the yields of oil and styrene monomer can be seen in Fig. 11. In the figure, the values of Y_{oil} and Y_{SM} attain 95.3 and 72.0%, respectively, when the reaction temperature is 450 °C without swirling gas. Note that the injection of swirling gas ($V_2/V_1 = 0.3$) increase the values of Y_{oil} and Y_{SM} up to 96.7 and 73.7%, respectively, at the same reaction temperature. However, the increase of reaction temperature from 450 to 550 °C cannot increase the values of Y_{oil} as well as Y_{SM} in using Fe_2O_3 catalyst, although the values tend to increase slightly with increasing reaction temperature in using BaO catalyst or without catalyst. Thus, it can be sound to state that the optimum reaction temperature is 450 °C

for the recovery of oil and styrene monomer from polystyrene waste within this experimental conditions.

5. Conclusion

The styrene monomer and valuable chemicals have been effectively recovered by employing the swirling fluidized-bed reactor. The temperature fluctuations have been utilized successfully as its state variable by adopting the chaos theory, to analyze the thermo-physical flow behavior in the reactor. The yields of oil products and styrene monomer increase with increasing the ratio of swirling gas, but exhibit local maxima with increasing total gas flow rate. The catalyst of Fe_2O_3 has been preferred to BaO or HZSM-5 for the increase in yields of oil product and styrene monomer. The optimum reaction temperature has been found to be 450 °C. And the optimum condition of reaction time (t), total gas volume flow rate (V_o) and swirling gas ratio (V_2/V_1) are 20 min, 3.6 m^3/h and 0.5, respectively, within this experimental conditions.

Acknowledgements

Financial support from Industrial Waste Recycling R&D Center (project A-B-1) has been greatly appreciated.

References

[1] F. Sasse, G. Emig, Chem. Eng. Technol. 21 (1998) 777.
[2] T. Hirose, Y. Takai, N. Azuma, Y. Morioka, A. Ueno, J. Mater. Res. 13 (1998) 77.
[3] J. Mertin, A. Kirsten, M. Predel, W. Kaminsky, J. Anal. Appl. Pyrol. 49 (1999) 87.
[4] B. Formisani, R. Girimounte, G. Pataro, Powder Technol. 125 (2002) 28–38.
[5] J. Zhang, S. Nieh, Powder Technol. 112 (2000) 70.
[6] B. Sreenivasan, V.R. Raghavan, Chem. Eng. Process. 41 (2002) 99.
[7] R.S. Miller, J. Bellan, Energy and Fuels 12 (1998) 25.
[8] C.H. Lin, J.T. Teng, C.S. Chyang, Combust. Flame 110 (1997) 163.
[9] J.K. Lee, C.G. Hu, J.G. No, Y.S. Shin, H.S. Chun, Hwahak Konghak 26 (1988) 517.
[10] J. Zhang, S. Nieh, Fuel 76 (1997) 123.
[11] Y. Kang, K.J. Woo, M.H. Ko, Y.J. Cho, S.D. Kim, Korean J. Chem. Eng. 16 (1999) 784.
[12] J. Drahos, F. Bradka, M. Puncochar, Chem. Eng. Sci. 47 (1992) 4069.
[13] K. Kuramoto, A. Tsutsumi, T. Chia, Can. J. Chem. Eng. 77 (1999) 291.
[14] J.C. Roux, R.H. Simoyi, H.L. Swinney, Physica D 8 (1983) 257.
[15] L. Huilin, D. Gidaspow, J.X. Bouillard, AIChE Symp. Ser. 91 (1995) 103.
[16] N.H. Packard, J.P. Crutchfield, J.D. Garmer, R.S. Shaw, Phys. Rev. Lett. 45 (1980) 712.
[17] J.S. Kim, S.J. Kim, J.S. Yun, Y. Kang, M.J. Choi, Hwahak Konghak 39 (2001) 465.
[18] C.G. Lee, J.S. Kim, P.S. Song, Y.J. Cho, Y. Kang, M.J. Choi, Hwahak Konghak 40 (2002) 445–449.
[19] Y.J. Cho, S.J. Kim, S.H. Nam, Y. Kang, S.D. Kim, Chem. Eng. Sci. 56 (2001) 6107.
[20] C. Lee, Y. Cho, P. Song, Y. Kang, M. Choi, Proceedings of the APCChE, September 29–October 3, New Zealand, 2002.
[21] O.S. Woo, L.J. Broadbelt, Catal. Today 40 (1998) 321.
[22] Z. Zhang, T. Hirose, S. Nishio, Y. Morioka, N. Azuma, A. Ueno, H. Ohkita, M. Okada, Ind. Eng. Chem. Res. 34 (1995) 4514.
[23] P. Carniti, A. Gervasini, P.L. Beltrame, G. Audisio, F. Bertini, Appl. Catal. 127 (1995) 139.
[24] S.D. Kim, Y. Kang, Chem. Eng. Sci. 52 (1997) 3639.